2026 IEEE International Conference on Robotics and Automation (ICRA 2026)
June 1-5, 2026. Vienna, Austria

The translational/ rotational piezoelectric impact drive mechanism for cell/tissue extraction from mouse cranial window

Hirotaka Sugiura[1], Hiroki Kunii[1], Satoshi Amaya[1], Shuntaro Kawamura[3], Takanori Takebe[345], Fumihito Arai[12]

***Abstract*— We developed a microscopic cell/tissue extraction device that employed a translational/rotational piezoelectric impact drive mechanism (Piezo IDM). To perform the correlation between gene expression and localized tissue sample at the micrometer scale, the system inserted a knife-edged glass capillary driven by the Piezo IDM and extracted the cells/tissues. The hybridized use of the translational and rotational impact motion significantly improved suction performance, resulting in the reliable acquisition of small, localized cells and tissues, which were previously difficult to be isolated. To characterize the motion of the Piezo IDM, the amplitude and frequency dependence were measured, and were compared with the simulation model. In addition, we found that the synchronous chopping motion could exert the rotational motion efficiently. For the automation, a specialized controller was developed to exert bidirectional motion. The experimental demonstration was performed for both the artificial gel sample and the practical mouse cranial window (CW). The result of the gel sample clearly exhibited the effectiveness of hybridizing the translational and rotational motion of Piezo IDM for cell/tissue extraction. The practical demonstration of the neutrophil extraction experiments in thrombus-induced mice also elucidated the potential performance of the accurate tissue extraction from the *in-vivo* environment.**

I. Introduction

Precise tissue extraction method at a microscopic scale is now essential to study the genetic analysis of the disease [1, 2]. Particularly, by using the emergent technique to incubate organoids, which express the characteristics of the organ and the relevant diseases in the genetic scale, the order and the mechanism of the disease become increasingly clarified [3, 4]. By extracting localized cell populations from these organoids, it becomes possible to significantly correlate with gene expression patterns and the disease progression in the three-dimensionally cultured organ models [5]. Indeed, conventional *in-vitro* systems could not perform the functional blood perfusion, limiting their physiological relevance. The method is now further refined to establish vascularized organoid models by embedding human-derived organoids into the cranial window (CW) of mice, enabling real-time, *in-vivo* analysis of human blood vessels and disease dynamics [6,7]. The CW provides a unique interface for both imaging and direct tool access to implanted organoids. This setup offers the possibility not only to observe disease-related tissue changes, such as thrombus formation, but also to extract specific cells for successive gene analyses. Such approaches will contribute

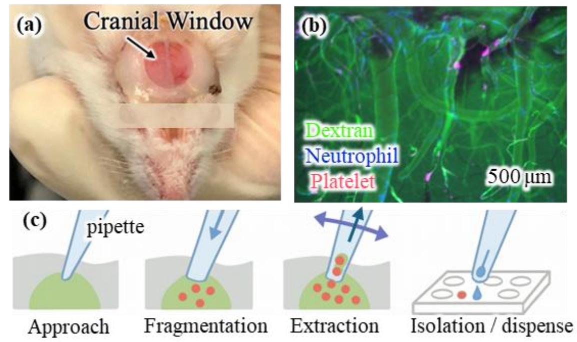

Fig. 1(a) Mouse cranial window; (b) Thrombus formation under fluorescent observation; (c) The procedure of the cell/tissue extraction and isolation.

to the discovery of pathogenic genes involved in thrombotic microangiopathy, sinusoidal obstruction syndrome, and other rare vascular disorders. For example, some models transplant human liver bud organoids onto immunodeficient mouse brains for blood supply and elucidated that the blood flow began, supplying nutrients and oxygen, and it grew into a tissue with liver-like functions [8]. These are quite useful techniques to understand the pathophysiology of vascular diseases that interacts deeply with human organs.

For gene expression analysis of these tissues, high-precision cell/tissue extraction tools are required. Previous reports such as Image-seq [9] and DISCO-bot [10, 11] demonstrated the local cell/tissue extraction, including perfused or cleared postmortem mouse brains. The sampling of the cell/tissue was examined only for the euthanized mouse, whose mechanical properties are corrupted and relatively easy for the tissue aspiration. Contrary, the blood supplies were already stopped, mentioning that the method could not trace and aim the growing spot of the vascular disease. The applications for living tissues, having the *in-situ* blood supply in the CW remains largely unexplored. For this reason, our group once examined a tissue sampling system using translational piezo IDM under microscopy [12]. The device consisted of the glass micropipette driven by the Piezo IDM and exhibited the good perforation ability to access the aimed cell/tissue, suppressing the viscoelastic deformation of the tissue. However, since the micropipette would not have sufficient aspiration force for tissue extraction, the sample collection was still quite challenging.

Corresponding: H Sugiura, hsugiura965@g.ecc.u-tokyo.ac.jp
1 Department of Mechanical Engineering, The University of Tokyo, Japan
2 Department of Bioengineering, The University of Tokyo, Japan
3 Human Biology Research Unit, Institute of Integrated Research, Institute of Science Tokyo, Japan
4. Department of Genome Biology, Graduate School of Medicine, and Premium Research Institute for Human Metaverse Medicine (WPI-PRIMe), the University of Osaka, Japan
5 Division of Gastroenterology, Hepatology and Nutrition & Division of Developmental Biology, Cincinnati Children's Hospital Medical Center, USA

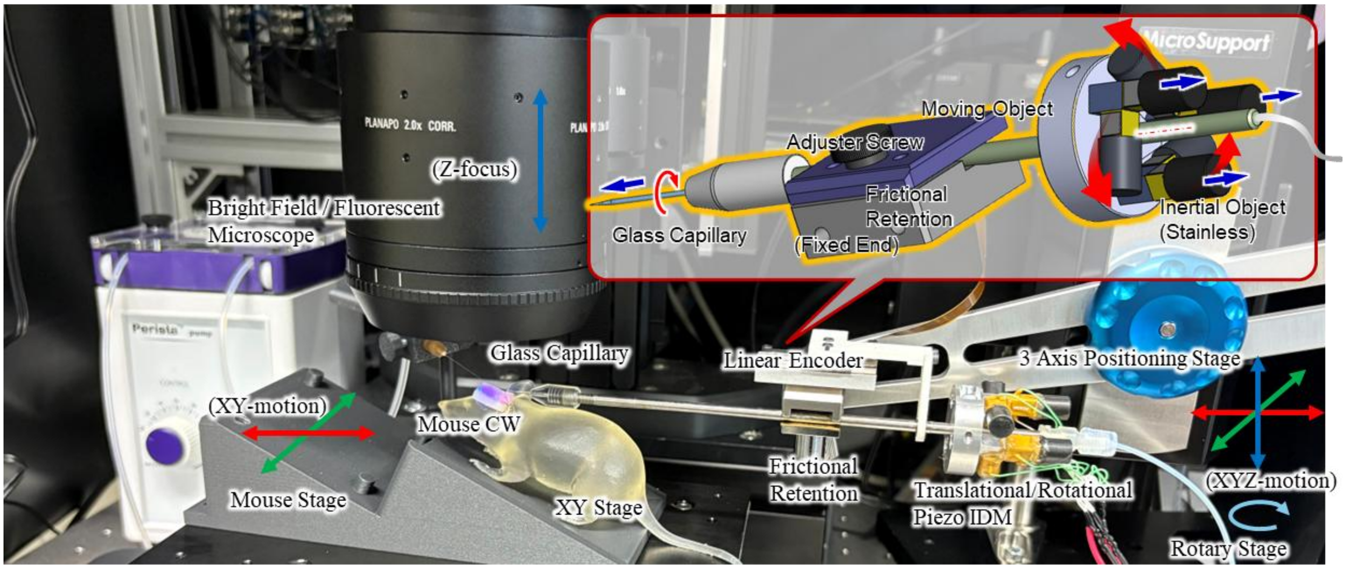

Fig. 2 The system overview of the cell/tissue extraction on the mouse CW by using Translational and Rotational Piezo IDM device. Notice that the mouse was changed to the 3D-printed model due to the ethical issue.

To overcome this issue, we propose a hybridized actuation method of the translational/rotational Piezo-IDM that applies rotational impacts during aspiration. Using a knife-edged glass capillary, we demonstrate successful gel sample extraction [13], highlighting the potential of the system for precise cell/tissue extraction inside the viscoelastic tissues. For more practical applications, we further characterize the performance and demonstrate cell/tissue extraction from real mouse CW, which was never realized in previous research. The main contributions of this paper are as follows.

- Translational and Rotational motions of the Piezo-IDM are superposed in a single device, making it possible to both the rotational motion of the tip of the knife-edged glass capillary to cause the shear force and the twisting extraction of the target cell/tissue.
- The experimental performance of the Piezo IDM was characterized, accounting for the amplitude and frequency dependence, and the response was modeled with the simple model parameters.
- The synchronous control of the translational motion and the rotational motion is realized by the specialized driving waveform generator.
- Successful tissue extraction was demonstrated by both the gel sample for quantitative analysis and the thrombus-induced mouse models to verify the potential of the system.

This work lays the fundamental architecture for high-precision, less invasive, localized gene profiling of disease-relevant tissues in live animal models.

II. System Configuration

An overview of the developed cell extraction system was illustrated in Fig. 2. The system was designed to perform micrometer-scale cell/tissue extraction from live tissue with precise spatial targeting and minimal damage. It consisted of the Translational/Rotational Piezo IDM that had a knife-edged glass capillary at the tip for tissue penetration, a syringe pump (Legato110/Harverd Bioscience Inc.) for tissue suction, a three-axis positioning stage (Quick Pro/Microsupport Co., Ltd.) combined with a rotary stage (OSMS-YAW120/ Sigma Koki Co., Ltd.) for IDM alignment, and an XY stage (OSMS26-100XY/ Sigma Koki Co., Ltd.) for positioning the mouse and fastening the mouse specimen. These were placed under a bright field and fluorescent microscope (Thunder/Leica microsystems Co., Ltd.) for the imaging of the target tissue with the fluorescent label. The mouse was held under the microscope, and the sample tissue like an organoid was embedded within a cranial window for direct optical access and continuous observation. In order to provide saline solutions for mouse CW, the peristatic pump (SJ-1211/Atto Corp.) and tube with the needle were placed next to the mouse. The mouse fixation jig was fabricated with the 3D-printed material.

The Translational/Rotational Piezo IDM was designed and fabricated by our laboratory. The basement was the stainless pole and the aluminum circular plate fastened by the screw clamp strongly. Three pieces of the piezoelectric stack actuators (PC4QM/Thorlabs Inc.) were attached for each of the translational and rotational orientations. The steel inertial bodies with the weight of 3.9 g were bonded at the tip of the piezo actuator. At the end of the stainless pipe, the fitting attachments of the glass capillary and the suction tube were connected. The glass capillary was fabricated by the thermal puller and the grinder (Narisige Co., Ltd.) to form the sharp needle edge. The size of the capillary tip was iteratively checked manually, until the size of the pipette tip became 200 μm. The stage position was measured by the photoreflection encoder (TA200, Technohands Co., Ltd.) to detect the relative displacement and facilitate the feedback control. These were fixed to the three-axis positioning stage via a frictional retention structure.

When operating the system, the fluorescent microscope was first used to identify the disease-relevant region or specific target cells inside the tissue. Once the target location was

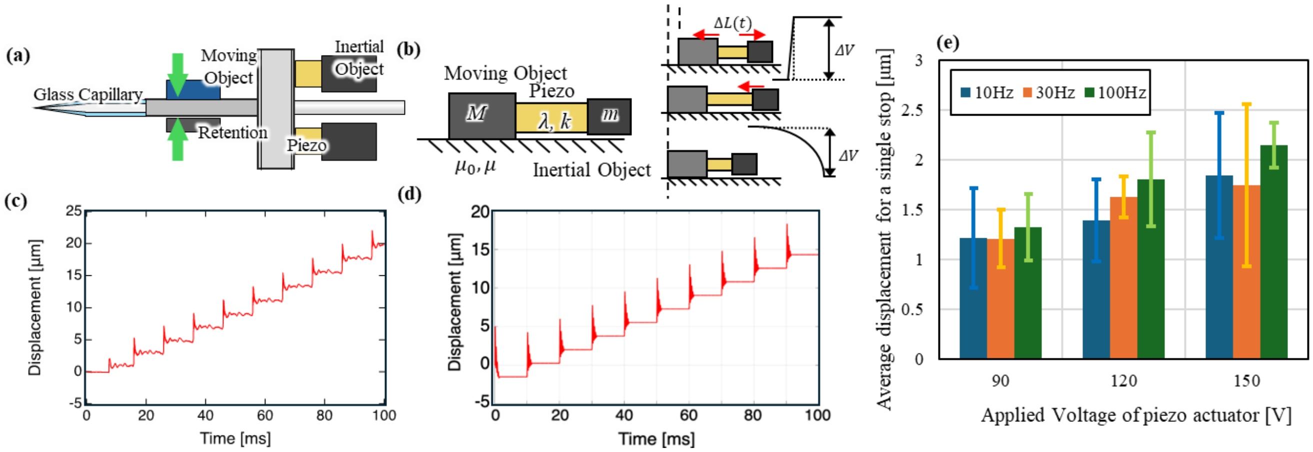

Fig. 3 The simplified model of the Piezo IDM and its comparison of the experimental results and simulation; (a)Structure of IDM, (b) Simplified driving model of the Piezo IDM motion; (c) A representative result of the displacement exerted on the Piezo IDM; (d) Simulation results of the Piezo IDM motion to presume the controllability of the device. (e)Parameter dependence of the Piezo IDM according to the amplitude and the frequency.

determined, the Piezo IDM was manipulated via the positioning stages to insert the angled glass capillary into the tissue at a precise orientation. Negative pressure was subsequently applied using the syringe pump to extract the tissue and draw it into the capillary tip. Finally, rotational motion was applied by the Piezo IDM to cause the shear force and collect the engaged tissue segment into the pipette without damaging surrounding structures. This integrated setup achieved site-specific localized tissue extraction with high spatial resolution, The latter section illustrate the performance of the device in further detail.

III. PIEZO IMPACT DRIVE MECHANISM (PIEZO IDM)

To quantitatively express the model of the Piezo IDM, as shown in Fig. 3(a), we account for a synthetic piezoelectric element, the basement, and the inertial body. As shown in Fig. 3(b), the actuation scheme is based on a cyclic combination of two motions: a slow extension/contraction of piezoelectric element exerted by the constant acceleration input and the rapid contraction/extension caused by the step input. This asymmetric motion generates directional displacement of the moving object due to inertial effects.

The simplified system of the piezo IDM is modeled by the following equations of motion that describe the interactions between the inertial mass and the moving object. The representative equations used in this study are as follows:

Inertial object

$$m\ddot{x} = -\lambda(\dot{x} - \dot{X}) - k(x - X - \Delta L(t)) \quad (1)$$

Moving object (static state / dynamic state)

$$M\ddot{X} = 0 \quad (2)$$

$$M\ddot{X} = \lambda(\dot{x} - \dot{X}) - k(x - X - \Delta L(t)) - \mu(M + m)g \cdot \mathrm{sign}(\dot{X}), \quad (3)$$

where, m and x represent the mass and the relative displacement of the inertial body, M and X represent those of the moving body, λ is the damping coefficient, k is the spring constant of the piezoelectric actuator, respectively. $\Delta L(t)$ is the time-dependent elongation of the piezo element. To characterize the mechanical behavior, we first recorded the actuation behavior experimentally using a high-speed camera and analyzed the resulting motion field using optical flow techniques of the OpenCV4 with the high-speed camera (Phantom/ Nobbytech Co., Ltd.). The piezoelectric actuators were driven by the function generator (Tektronix Inc.) and the piezo amplifier (M26109/Messtek Co., Ltd.). The experimentally observed displacement were depicted in Fig. 3(c). As illustrated in the acute edge of the response, the pulsed displacement was generated, which contributed to the smooth injection of the glass pipette. By the iterative parameter adjustment of the Piezo IDM, the numerical simulation results also showed the consistent response as expressed in Fig. 3(d). These models could be in accord with both the translational and rotational orientation. From this model, we could simulate the effect of the preferable pulse generation. The model parameters were $m = 3.0 \times 10^{-2}\ kg$, , $M = 5.0 \times 10^{-2}\ kg$, , $\lambda = 50\ N \cdot m/s$, $k = 7 \times 10^6$ N/m, $\mu = 3, \mu_0 = 20$, respectively.

Figure 3(e) represents the dependence of the input amplitude and the frequency. The driving region was from 90 V to 150 V, from 10 Hz to 100 Hz. The result illustrated that the amplitude was proportional to the amplitude of the input step, whereas the frequency was not principally related to the performance with no load at the tip of the device. The frequency dependence might be attributed to the properties of the target tissue, since the relaxation of the sample would be comparable to the time scale. This issue will be addressed in our future work, when we deal with the general sample as a target of the cell/tissue extraction. In this study, in the light of the efficient stroke generation and small deviation of the indentation displacement, we utilize 100 Hz as an operation frequency of the Piezo IDM.

Using the amplitude dependence of the actuator, the implementation of the Piezo IDM was modified from open-loop mode to feedback mode. As the stroke generated by each actuation cycle had considerable standard deviation, the repeatability of the positioning had a challenge for precise motion control. Therefore, the feedback control was essentially implemented using the optical encoder. This is explained in the later experimental section.

IV. Extension of Translational/Rotational Motion

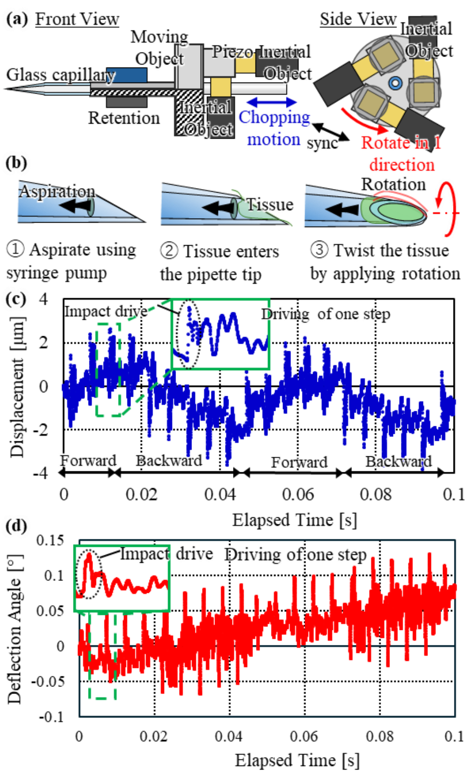

Fig. 4 The extension of the Piezo IDM toward the rotational axis; (a) Structure to exert the translational and Rotational Motion; (b) the knife edge of the pipette tip; (c) relative translational displacement and (d) the deflection angle.

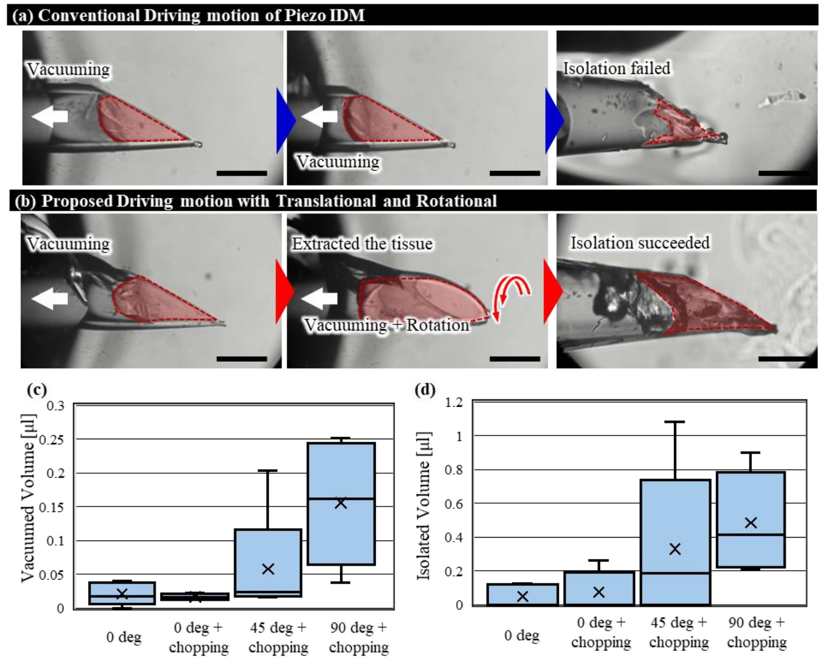

Fig. 5 The characterization of the tissue extraction; (a-b) The experimental image to extract the local gel sample with and without the rotational motion. The rotational motion definitely improve the extraction volume due to the twisting fragmentation, the scale bar was 50 µm; (c) The vacuumed volume at the pipette tip under suction and (d) Finally isolated volume of the tissue, which was the remaining volume of the tissue after retraction of the pipette from the tissue.

To improve tissue extraction efficiency under viscoelastic conditions, we developed a novel actuation mode that extends the conventional translational Piezo IDM by adding a rotational driving function. The structure of the developed Translational/Rotational Piezo IDM is illustrated in Fig. 4(a). As with the previous design, the mechanism employed piezoelectric actuators were driven by the asymmetric waveform. The principle of tissue sampling using this mechanism is shown in Fig. 4(b). A glass capillary with a 30° knife-edge tip was inserted into the target tissue. Upon applying negative pressure, the soft biological material was deformed and was partially drawn into the capillary tip. The superimposed rotational motion generated by the actuator caused the engaged tissue to twist and shear, resulting in a fragmentation of tissue and aspiration into the pipette. This hybridized motion was essential for achieving cell/tissue extraction in living tissue, where only simple suction was insufficient due to high tissue elasticity.

To generate the desired rotational behavior, simultaneous translational motion was required. We implemented a motion pattern in which the actuators oscillated back and forth while gradually introducing rotational torque. This is what we call “chopping motion”, to further accelerate the fragmentation of the highly viscoelastic tissue and keeping the contact region of frictional retention as a dynamic friction, to cause smooth rotation. The representative response of the response are depicted in Fig. 4(c-d). This coordinated motion strategy was key to achieving successful extraction of micro-scale tissue regions without causing large-scale mechanical damage.

To characterize the performance of the developed cell extraction system, we examined suction experiments using a viscoelastic polymer material instead of live biological samples. This was necessary because maintaining the physiological condition of a mouse CW in a controlled experimental environment is technically demanding, making it difficult to quantitatively characterize the performance of the device. Moreover, imaging under a fluorescent stereomicroscope offers limited brightness and resolution, making it difficult to observe and quantify the deformation and extraction behavior of biological tissues in detail. To avoid these issues, we used an alternative, KE-1013 (Shin-Etsu Chemical Co., Ltd.), a liquid silicone rubber with properties suitable for mimicking soft biological tissue. To enhance the visibility of deformation and internal motion, we mixed the silicone with a small amount of graphite carbon (Merck KGaA), which provided visual contrast under optical microscopy.

The imaging setup was configured upon an upright optical microscope equipped with a high-speed camera, for high-speed visualization of the suction and extraction process. To further facilitate clear observation, the experimental configuration was arranged so that the micropipette was aligned parallel to the objective lens, while the polymer sample was tilted diagonally to expose the insertion path of the capillary. Figure 5(a) illustrates the difference in sample extraction

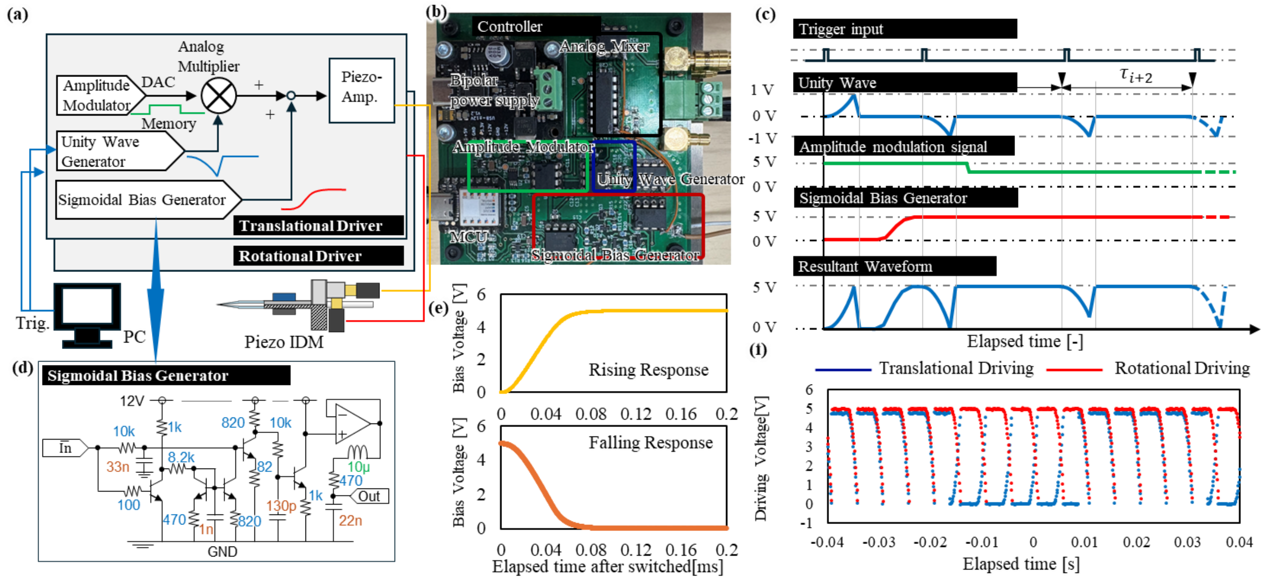

Fig. 6(a) The overview of the controller to exert the translational and the rotational motion of Piezo IDM with real-time orientation switch and amplitude modulation; (a) The schematic of the controller; (b) The picture and function of the controller; (c) An example of waveform generation; (d) The schematic of the sigmoidal bias generator; (e) The step-response of the sigmoidal bias generator; (f) The experimentally generated waveform when the chopping motion was exerted.

between two driving modes of Piezo IDM, pure translation versus combined translation and rotation. When using only translational motion, the polymer sample deformed but was not successfully isolated from the surrounding matrix. However, when rotational motion was added, the sample at the tip of the glass capillary experienced torsional stress, which effectively facilitated separation and extraction. This demonstrated the importance of rotational shearing in achieving biopsies from viscoelastic media. To quantitatively evaluate the effect of rotational motion, we examined the extracted volume as a function of the rotational angle of the Piezo IDM. Fig. 5(c) shows the volume of the polymer drawn into the glass pipette at various rotation angles. To isolate the effects of rotation, we also examined control experiments at 0° with and without translational chopping. The results clearly suggested that suction without rotation resulted in minimal volume uptake. As the rotation angle increased, the extracted volume grew significantly, indicating that rotational shear force or twisting fragmentation, resulting in successful tissue separation.

Figure 5(d) presents the volume remaining inside the capillary after extraction and withdrawal of the glass pipette, again plotted against the rotation angle. The trend was consistent with the pre-withdrawal results: very little material remained in the absence of rotation. In contrast, larger volumes were observed at higher rotation angles. It also suggested that the volumes in Fig. 5(c) were greater than those in Fig. 5(d), mentioning that additional tissue was often drawn in during the pipette retraction. This phenomenon is due to continued suction applied during withdrawal, causing the pipette to scoop up surface material from the polymer sample. Overall, these experiments confirm that combining rotational and translational motions resulted in effective sample extraction from viscoelastic gel sample, that shows the sufficient potential for the *in-vivo* applications.

V. Tissue Extraction from Mouse CW

A. The controller configuration

In order to implement the Translational/Rotational motion of the Piezo IDM into the experimental system, the control command should be interpreted to the driving signal of the Piezo IDM. Given that the chopping motion, cyclic indentation and retraction of the translational motion and the steady rotational motion, required the switching of the orientation, one preferable baseline of the driving voltage could be half of the rated driving voltage of 150 V. On the other hand, as the previous characterization illustrated, the indentation depth could be controlled by the amplitude of the voltage signal from 90 V to 150 V. It mentioned that the baseline should be switched depending on the orientation change, suppressing the motion of the Piezo IDM. To meet this unique requirement, we fabricated a specialized controller as shown in Fig. 6(a). The controller had the unity wave generator to create the IDM driving signal with constant acceleration and sudden step-back. The signal had orientation information as a bipolar signal. By mixing the unity wave with the voltage signal from DA converter, the amplitude could be modulated to realize the precise positioning. In addition, the sigmoidal bias generator was also configured as an analogous circuit. This circuit could exert the sigmoidal step signal within 100 μs, suppressing the sudden acceleration and deceleration. Therefore, this signal could be inserted between the interval of the IDM driving signal when the orientation was switched. The whole architecture of the controller was designed as depicted in Fig. 6(b) and some examples of the waveform generation was illustrated in Fig. 6(c). The sigmoidal bias generator was designed by using the discrete transistor to suppress the delay of the output for real-time control as depicted in Fig.6 (d). The circuit was configured by the RLC low-pass filter, and acceleration and deceleration was controlled by the active low-pass filter and the current mirror circuit. The practical transient

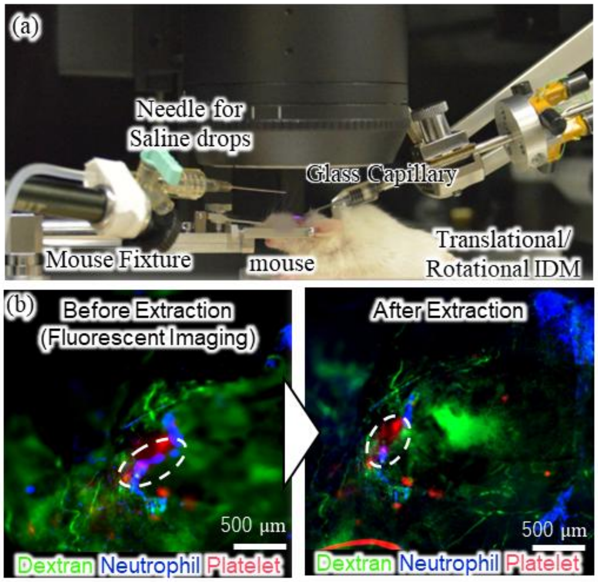

Fig. 7(a) An overview of the cell/tissue extraction from the mouse CW; (b) The experimental results when a specified single neutrophil and the surrounding tissue was extracted from the tissue.

response of the sigmoidal waveform generator was illustrated in Fig.6(e). The representative driving signal was illustrated in Fig. 6(f). Using this controller, we addressed the specified target cell. The control algorithm is just a simple proportional control.

B. *Extraction of localized neutrophil and tissue*

The developed system was tested in a mouse model to validate its capability for in-vivo cell extraction. The experimental setup is illustrated in Fig. 7(a). A mouse CW was surgically prepared in the mouse skull to allow direct access to the brain surface. Lipopolysaccharide (LPS) was administered systemically to induce thrombus formation prior to the procedure. During the experiment, the mouse was kept under deep anesthesia, and saline was continuously applied to the exposed brain surface to maintain physiological conditions. To facilitate real-time observation, fluorescently labeled dextran was injected intravenously, enabling visualization of blood vessels. Additionally, fluorescently labeled anti-Ly6G and anti-CD41 antibodies were administered to identify neutrophils and platelets, respectively. As shown in Fig. 7(b), fluorescence imaging clearly revealed neutrophil accumulation around thrombi. Target neutrophils were identified as highlighted with white circles. and extracted using the developed piezo-driven micromanipulation system. The extraction damage was carefully reduced to surrounding tissues. The success of extraction was further confirmed through RNA quantification of the harvested sample, yielding 131 ng of total RNA. The current issue was that the extracted sample would have the impurities preventing the gene expression analysis of the aimed cell like neutrophils. Therefore, the secondary extraction process was necessary to increase the purity of the aimed sample. Depending on the requirement of the spatial resolution of the sample, the proposed method still exhibited the potential for the localized cell/tissue analysis, and the performance will be further updated in near future.

VI. Conclusion

In this study, we developed an *in-vivo* single-cell extraction system capable of isolating target cells from live mouse brain tissue with high precision. Through experiments using polymer gel samples, we demonstrated that the combination of suction via syringe pump and rotational motion of the IDM enabled successful penetration and extraction even from viscoelastic tissue. Furthermore, the extraction efficiency was shown to depend on the rotation angle, highlighting the importance of motion control. RNA analysis of the collected sample validated the success of extraction. These results indicated that our system exhibited a promising platform for minimally invasive, spatially precise tissue sampling for downstream molecular analysis.

Acknowledgment

This work was supported by JST Moonshot R&D - MILLENIA Program Grant Number JPMJMS2033-08.

References

[1] D. J. Birnbaum, S. K. S. Begg, P. Finetti,…, “Transcriptomic analysis of laser-capture microdissected tumors reveals cancer- and stromal-specific molecular subtypes of pancreatic ductal adenocarcinoma,” *Clin. Cancer Res.*, vol. 27, no. 8, pp. 2314–2325, 2021.

[2] F. Scala, D. Kobak, M. Bernabucci, Y. Bernaerts, C. R. Cadwell,…, “Phenotypic variation of transcriptomic cell types in mouse motor cortex,” *Nature*, vol. 598, no. 7879, pp. 144–150, 2021.

[3] J. G. Camp, F. Bedsha, M. Florio, S. Kanton, T. Gerber, …, “Human cerebral organoids recapitulate gene expression programs of fetal neocortex development,” *Proc. Natl. Acad. Sci. USA*, vol. 112, issue 51, pp. 15672-15677, 2015.

[4] G. Quadrato, T. Nguyen, E. Z. Macosko, J. L. Sherwood, …, “Cell diversity and network dynamics in photosensitive human brain organoids,” *Nature*, vol. 545, pp. 48–53, 2017.

[5] K. Ye, Y. Guo, N. Chang, J. Xu, Q. Qin, X. Yang, Y. Huang, …, “Micro-region transcriptomics profiling of cerebral organoids using a capillary-based microdissection system,” *Anal. Methods*, vol. 17, no. 17, pp. 3480–3489, 2025.

[6] A. A. Mansour, J. T. Gonçalves, C. Bloyd, D. Li, S. Fernandes, C. Quang, D. Johnston, and A. H. Gage, “An in vivo model of functional and vascularized human brain organoids,” *Nat. Biotechnol*., vol. 36, no. 5, pp. 432–441, 2018.

[7] T. Takebe, K. Sekine, M. Enomura, H. Koike, T. Kimura, …, “Vascularized and functional human liver from an iPSC-derived organ bud transplant,” *Nature*, vol. 499, no. 7459, pp. 481–484, 2013.

[8] S. P. Harrison, R. Siller, Y. Tanaka, M. E. Chollet, M. E. …“Scalable production of tissue-like vascularized liver organoids from human PSCs,” Exp. Mol. Med., vol. 55, pp. 2005–2024, 2023.

[9] C. Haase, K. Gustafsson, S. Mei, M. L. Grzybowski, …, “Image-seq: spatially resolved single-cell sequencing guided by in situ and in vivo imaging,” Nat. Methods, vol. 19, no. 12, pp. 1622–1633, 2022.

[10] M. Molbay, Z. I. Kolabas, M. I. Todorov, …, “A guidebook for DISCO tissue clearing,” Mol. Syst. Biol., vol. 17, no. 3, e9807, 2021.

[11] H. S. Bhatia, A.-D. Brunner, F. Öztürk, J. F. Hoppe, …, “Spatial proteomics in three-dimensional intact specimens,” Cell, vol. 185, no. 26, pp. 5040–5058.e19, 2022.

[12] H. Kunii, H. Sugiura, S. Amaya, and F. Arai, “Smooth pipette-tool insertion for the single cell pickup using piezoelectric impact driving mechanism,” *Proc. International Symposium on Micro-NanoMechatronics and Human Science (MHS2024)*, Nagoya, 2024.

[13] H. Kunii, H. Sugiura, S. Amaya, F. Arai, “THE MICROSCOPIC BIOPSY DEVICE FOR THE HIGHLY VISCOELASTIC TISSUE BY USINGTRANSLATIONAL/ROTATIONAL PIEZO IMPACT DRIVE MECHANISM,” *Proc IEEE Transducers 2025*, Orlando, USA, 2025